Isolation and characterization of topological specificity mutants of minD in Bacillus subtilis

Molecular Microbiology (2001) **42**(5), 1211–1221

Isolation and characterization of topological specificity mutants of *minD* in *Bacillus subtilis*

M. El Karoui[†] and Jeffery Errington*
Sir William Dunn School of Pathology, University of Oxford, Oxford OX1 3RE, UK.

Summary

In rod-shaped bacteria such as *Bacillus subtilis*, division site selection is mediated by MinC and MinD, which together function as a division inhibitor. Topological specificity is imposed by DivIVA, which ensures that MinCD specifically inhibits division close to the cell poles, while allowing division at mid-cell. MinD plays a central role in this process, as it positions and activates MinC and is dependent on DivIVA for its own positioning at the poles. To investigate MinD activities further, we have constructed and analysed a collection of *minD* mutants. Mutations in the conserved ATPase motifs lead to an inactive protein, possibly unable to oligomerize, but which nevertheless retains some affinity for the cell membrane. Several mutations affecting the mid- to C-terminal parts of MinD led to a protein probably unable to interact with DivIVA, but that could still stimulate division inhibition by MinC. These findings suggest that the ATPase activity of MinD is necessary for all its functions (possibly in part by controlling the oligomerization state of the protein). The other mutations may identify a surface of MinD involved in its interactions with DivIVA and a possible mechanism for control of MinD by DivIVA.

Introduction

A fundamental problem in bacterial cell division is the nature of the mechanism that positions the division septum at the correct place in the cell. In rod-shaped bacteria, such as *Bacillus subtilis*, it is usually placed midway along the long axis of the cell, so that division gives rise to two daughter cells of equal size. The highly conserved tubulin-like protein called FtsZ, a central component of the division apparatus, forms a ring-like structure at the division site (Lutkenhaus and Addinall, 1997): correct mid-cell placement of the FtsZ ring is under the control of the MinCD/DivIVA system (MinCDE in *Escherichia coli*; see below). This system allows selection of the mid-point of the cell as the division site in preference to two other potential sites located close to the cell poles. Evidence that the poles are potential division sites comes from the minicell (*min*)-producing mutants: these mutants divide at approximately the normal frequency, but septation frequently occurs close to the cell poles, giving rise to small, spherical usually anucleate cells (Adler *et al*., 1967; Reeve *et al*., 1973; Teather *et al*., 1974).

MinC and MinD act together to inhibit cell division. Apparently, MinC is the actual inhibitor of assembly of the division apparatus, which functions by preventing FtsZ polymerization (Hu *et al*., 1999). MinD is required for MinC activity (de Boer *et al*., 1990; Marston and Errington, 1999) by a mechanism that is not yet clear but may involve enrichment of MinC at the cell periphery (where FtsZ ring assembly occurs) (Hu *et al*., 1999; Raskin and de Boer, 1999a). In *B. subtilis*, DivIVA protein is required to target the MinCD inhibitor to the cell poles. It is recruited to mid-cell late in cell division and then attracts MinD (and thus MinC) to this site. After division, DivIVA and MinCD remain at the newly formed poles, thus preventing division from occurring again at these sites. Moreover, by sequestering MinCD away from mid-cell, the next FtsZ ring assembly is free to occur at mid-cell. In the absence of DivIVA, MinCD spreads diffusely over the cell and prevents division from occurring anywhere in the cell, leading to filamentation and cell death (Cha and Stewart, 1997; Edwards and Errington, 1997; Marston *et al*., 1998; Marston and Errington, 1999).

In *E. coli*, the MinCD division inhibitor is controlled in a somewhat different manner. In this organism, DivIVA is not present, and a quite different protein, MinE, controls the topological specificity of MinCD (de Boer *et al*., 1989). This is achieved by a remarkable mechanism, in which MinD oscillates from pole to pole with a period of about 50 s in a MinE-dependent manner (Raskin and de Boer, 1999b; Rowland *et al*., 2000; Fu *et al*., 2001; Hale *et al*., 2001). MinC oscillates with the same pattern and frequency as MinD but is a passenger in the oscillation (Hu and Lutkenhaus, 1999; Raskin and De Boer, 1999a). In essence, the MinDE machinery seems to work by ensuring that MinC spends more time at the cell poles than at mid-cell.

MinD is highly conserved among bacteria: for example,

Accepted 11 September, 2001. *For correspondence. E-mail erring@molbiol.ox.ac.uk; Tel. (+44) 1865 275 561; Fax (+44) 1865 275 556. [†]Present address: Laboratoire de Recherches laitières et Génétique Appliquée, URLGA, INRA Centre de Jouy-en-Josas, 78352 Jouy-en-Josas cedex, France.

the *E. coli* and *B. subtilis* proteins share 44% identical residues. It is a member of a large family of ATPases of diverse functions (Koonin, 1993), which includes ParA and Soj, which are involved in plasmid and chromosome partitioning (Hiraga, 2000), and ArsA, which is the energy transducer for the transport of certain anions (Chen *et al.*, 1986). Sequence comparison of these proteins has allowed the identification of five conserved motifs (Gérard *et al.*, 1998) (Fig. 1), among which three are probably involved in the ATPase activity. The *E. coli* MinD protein has been purified and shown to be able to bind and hydrolyse ATP (de Boer *et al.*, 1991). Recently, the structures of two MinD proteins from *Archaeoglobus fulgidus* (Cordell and Löwe, 2001) and *Pyrococcus furiosus* (Hayashi *et al.*, 2001) were described. These structures appear to confirm the importance of the conserved motifs in ATP binding, but they did not shed much light on the functioning of the protein.

MinD appears to be a central component of the division site selection system, as it is an intermediate between the topological specificity factor and the division inhibitor in both *B. subtilis* and *E. coli*. This suggests that, in *B. subtilis*, it has several functions. First, an interaction with DivIVA, the topological specificity factor, which is responsible for proper MinD localization (Marston *et al.*, 1998), although a direct interaction has not been shown so far. Secondly, an interaction with MinC, the division inhibitor, which depends on MinD for its own localization and activation. Yeast two-hybrid experiments have demonstrated a direct interaction between MinC and MinD (Marston and Errington, 1999) (as in *E. coli*; Huang *et al.*, 1996). Thirdly, several lines of evidence suggest that MinD associates with the cell membrane: fluorescence microscopy indicates that most of the protein lies close to the cell envelope (Marston *et al.*, 1998), and electron microscopic studies of *E. coli* MinD suggest an inner

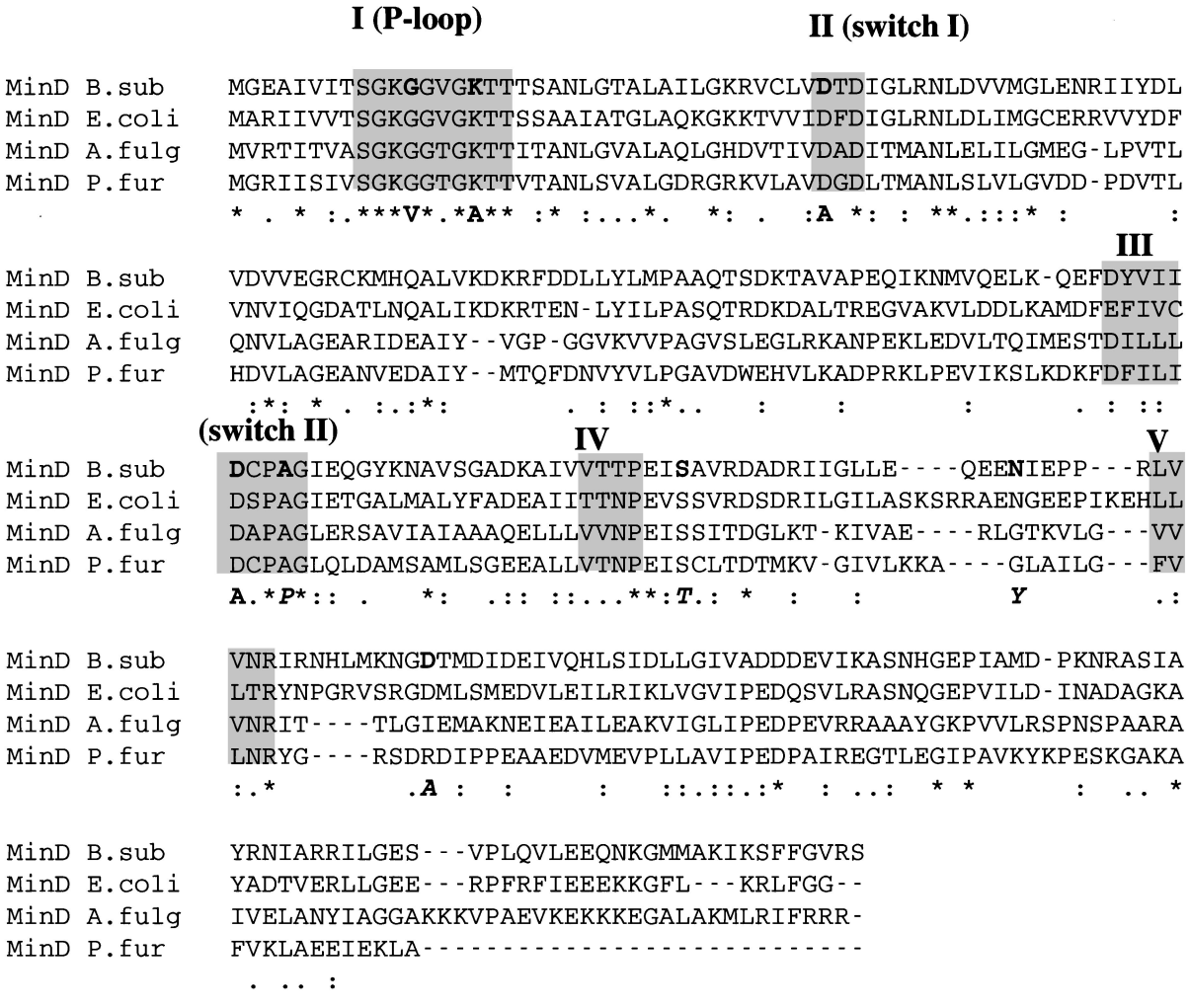

Fig. 1. Sequence alignment of *B. subtilis*, *E. coli*, *A. fulgidus* and *P. furiosus* MinD proteins (alignment obtained with CLUSTAL_W and edited manually; Thompson *et al.*, 1994). The five conserved motifs (Gérard *et al.*, 1998) are boxed. The amino acid changes are indicated below the alignment (bold letters, Min$^-$ mutants; bold and italic letters, Sep$^-$ mutants).

membrane localization (de Boer *et al*., 1991). A fourth possible activity might be inferred from the localization patterns of MinD in both *B. subtilis* and *E. coli*. In *B. subtilis*, the DivIVA protein to which MinD is attracted is targeted to small well-defined spots right at the cell poles (Edwards and Errington, 1997), whereas MinD occupies a much broader zone emanating some distance away from the cell pole (Marston *et al*., 1998). In *E. coli*, MinD oscillation appears to be co-operative, with most of the protein molecules being attracted to the same cell pole at any point in the oscillation cycle (Raskin and de Boer, 1999b; Rowland *et al*., 2000). Both kinds of behaviour suggest that MinD localization involves some kind of self-interaction to form oligomers or polymers. This has not yet been tested directly, although there is evidence for a weak MinD–MinD interaction from yeast two-hybrid studies (A. L. Marston, unpublished).

We have investigated MinD function further by site-directed and random mutagenesis. Mutations affecting the conserved ATPase motifs lead to an inactive protein, which nevertheless retains some affinity for the cell membrane. In contrast, several mutations affecting the middle and C-terminal parts of MinD lead to a protein probably unable to interact with DivIVA but that can still stimulate division inhibition by MinC. These findings suggest that the ATPase activity of MinD is crucial for all its functions. They also define a region of MinD that may be involved in its interaction with DivIVA and suggest a possible mechanism for sequestration of MinD.

Results

MinD localization and activity requires the conserved ATPase motifs

Of the conserved motifs identified by Gérard *et al*. (1998) (Fig. 1), motifs I and III are modified versions of the classical Walker 'A' and 'B' ATP-binding motifs (also called the 'P-loop' and 'switch II' sites). Motif II (switch I site) contains two conserved aspartate residues that are probably involved in the co-ordination of Mg^{2+} (Walker *et al*., 1982; Cordell and Löwe, 2001; Hayashi *et al*., 2001). We constructed four mutations in these three motifs. Two of them, K16A (i.e. lysine to alanine at amino acid 16) and D120A are predicted to disrupt ATP binding. Lysine 16 is nearly invariant in all Walker A boxes and interacts with the bound nucleotide (Story and Steitz, 1992). In ArsA, an ATPase homologous to MinD, the equivalent of aspartate 120 indirectly co-ordinates the magnesium ion in the ATP-binding pocket (Zhou *et al*., 2000). The third mutation, aspartate to alanine at amino acid 38 (D38A), probably decreases the affinity of the protein for Mg^{2+}: aspartate 38 is one of the two conserved aspartates in motif II. An equivalent amino acid in ArsA has been shown to be essential for the ATPase activity (Zhou and Rosen, 1999). The fourth mutation, glycine to valine at amino acid 12 (G12V), possibly alters nucleotide hydrolysis: the equivalent mutation in HA-ras p21 results in a protein that can bind GTP but has a greatly reduced rate of hydrolysis (Vogel *et al*., 1988). Western blot analysis indicated that all four MinD mutant proteins were produced at approximately wild-type levels (data not shown).

For all these mutant proteins, we tested MinD function and localization as well as MinC localization. The mutations were constructed by polymerase chain reaction (PCR) on a vector (pSG4801) carrying *minD* and a chloramphenicol resistance gene to allow selection (see *Experimental procedures*). The mutated copies of *minD* were introduced into the wild type strain (SG38) or into strains carrying a *gfp–minC* fusion (strain 2895; here *minD* is directly downstream of *gfp–minC*) or a *gfp–minD* fusion (strain 2896). The latter two recipient strains contain a deletion of *minCD* at the wild-type locus and the GFP fusions elsewhere on the chromosome driven by a xylose-inducible promoter (P_{xyl}). Although it does not have *minC,* strain 2896 allows the examination of MinD localization, which is known to be independent of MinC (Marston and Errington, 1999). Insertion of the plasmid was designed in such a way that only one functional copy of *minD* was present in the cell, i.e. the mutated copy. In the wild-type background (strains 2867–2869 and 2908), all four mutations produced phenotypes (designated Min^-) similar to those of null mutations: minicells accumulated, indicating that division was not inhibited at the poles. All the strains displayed a slightly reduced ability to sporulate (Levin *et al*., 1992; Lee and Price, 1993; Cha and Stewart, 1997; Barák *et al*., 1998), and the cell length was also slightly increased, as expected in a *minD* null mutant strain (data not shown). Thus, all four of these Min^- MinD proteins were impaired in their ability to mediate the inhibition of cell division.

Examination of GFP–MinD localization by fluorescent microscopy revealed that none of the mutant proteins was targeted to the cell poles. Instead, they were diffusely distributed along the length of the cell. Figure 2C shows an example of the typical staining pattern for one of the mutants (K16A) compared with the wild type (Fig. 2A); similar results were obtained with all the other mutants (data not shown). Fluorescence intensity line plots across the mutant cells (Fig. 2E) showed that the signal was apparently enriched at the periphery of the cell (indicated by the arrows), suggesting that these mutant proteins retain an affinity for the inner face of the cell membrane, as for the wild-type protein (de Boer *et al*., 1991; Marston *et al*., 1998). The transverse bands could correspond to recruitment of the mutant MinD proteins to impending or ongoing cell division events, in which case these proteins may retain some affinity for the division machinery

(Marston and Errington, 1999). More likely, the bands simply represent plates of membrane at division septa, lying perpendicular to the image plane.

Visualization of the intracellular localization of MinC with a GFP–MinC fusion indicated that it was also delocalized and distributed throughout the cell (Fig. 2D; compare with the wild-type pattern of localization in Fig. 2B), similar to *minD* null mutant strains (Marston and Errington, 1999). These images also showed the accumulation of minicells, as expected for a mutant in which MinD is inactive (Fig. 2A, arrow). Although difficult to detect against the background of dispersed protein, no increase in the GFP signal was evident at the cell periphery (Fig. 2F). Taken together with the Min$^-$ phenotype, this suggested that the interaction between MinC and MinD was disrupted in these mutants.

We also introduced mutations in motifs IV and V (V142A and N174A). However, the resulting mutant strains (2870 and 2871) did not have a detectable division placement defect, and localization of MinD and MinC was normal. This indicates that, although the two modified amino acids belong to conserved motifs, they are not essential for MinD activity (data not shown).

Together, these results suggest that ATP binding and possibly hydrolysis are essential for all MinD activities except for its affinity for the membrane.

Isolation of minD *mutants in which division is inhibited throughout the cell*

To investigate the nature of the proposed interaction between MinD and DivIVA involved in MinD targeting to the cell poles, we developed a screening system to isolate *minD* mutants in which MinD would no longer target to the poles but would retain the ability to activate MinC. As in a *divIVA* null strain (Cha and Stewart, 1997; Edwards and Errington, 1997), these mutants should grow poorly and be filamentous because cell division would be inhibited throughout the cell. To overcome this difficulty, we made use of strain 2895, in which *gfp–minC minD* is under the control of the P_{xyl} promoter. Introduction of a mutagenized *minD* gene by single cross-over into the chromosome of this strain would lead to a construct in which the mutated copy of *minD*, which is co-transcribed with *gfp–minC*, is controlled by P_{xyl} (a second wild-type copy of *minD* is present but not expressed). This allows the balanced ratio of MinC and MinD necessary for the proper functioning of the system (Marston and Errington, 1999). A mutation conferring the expected phenotype should lead to colonies growing very poorly in the presence of xylose but that can be rescued when grown without xylose (when they should simply have a classical minicell phenotype).

minD was randomly mutagenized by PCR and cloned in pSG1301 for integration by single cross-over in strain 2895 (see *Experimental procedures*). Of about 1500 transformants screened in the presence of xylose, four seemed to grow very poorly and appeared to be filamentous when examined by microscopy. All four candidates (Sep$^-$ mutants) carried mutations that would produce substitutions in the middle or C-terminal parts of MinD: A123P (*minD12*, strain 2912); S148T (*minD16*, strain 2916); N165Y (*minD15*, strain 2915); and D185A (*minD11*, strain 2911). The structure of the integration in each mutant was checked by PCR and appeared to be correct for all the strains except 2912. We used homologous recombination to construct a derivative of the *minD12* mutant in which the plasmid sequences were removed (see *Experimental procedures*). The resultant strain (2927) also carried *gfp–minC minD12* driven by P_{xyl},

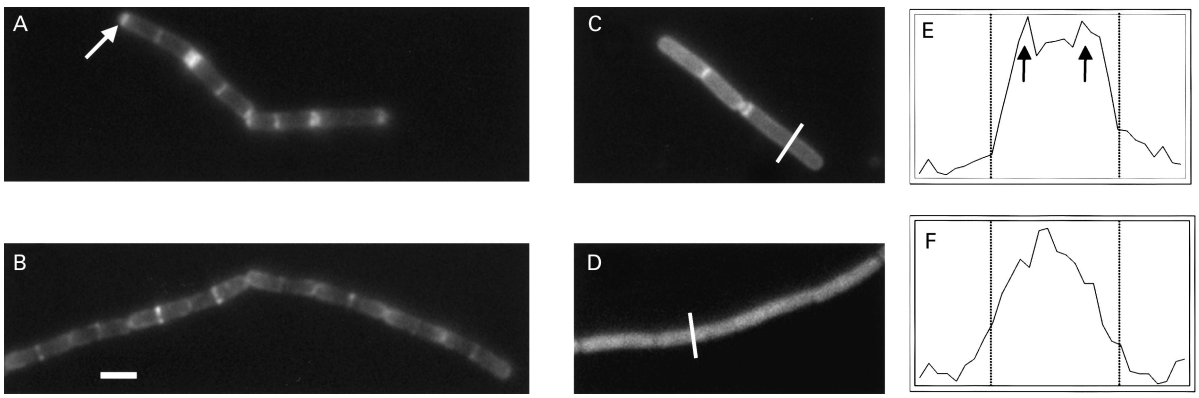

Fig. 2. Examples of the localization of GFP–MinD and GFP–MinC in a Min$^-$ mutant. Cells were grown to exponential phase (OD_{600} of 0.6–0.7) in S medium containing 0.5% xylose. Samples were taken for fluorescence microscopic imaging of the GFP.
A, C and E. Dispersed membrane distribution of GFP–MinD(K16A) (C, strain 2888) compared with wild-type GFP–MinD (A, strain 2893). (Note that these strains do not have *minC* and therefore produce minicells – arrowed in A.)
B, D and F. Diffuse cytoplasmic distribution of GFP–MinC in a *minD1* (K16A) mutant background (D, strain 2880) compared with a wild-type (*minD*$^+$) background (B, strain 2885).
E and F. Fluorescence intensity line plots across the cells in (C) and (D) respectively (at positions corresponding to the white lines in C and D). Scale bar (B) = 2 μm.

but it had a structure slightly different from the other mutant strains because only one copy of *minD* remained. This derivative proved to have the genetic structure expected and the correct *minD* DNA sequence. Western blot analysis showed that, when grown in the presence of xylose, all the Sep$^-$ mutants produced the mutated MinD protein at approximately wild-type levels (data not shown).

Sep$^-$ mutants are probably affected in DivIVA interaction

To confirm that division was inhibited in the mutants, we determined the cell length frequency distribution of exponentially growing cultures of strains 2911, 2915, 2916 and 2927 in the presence of xylose (in these conditions, the mutant MinD protein is produced). As shown in Fig. 3B–E, the cell length was increased in all Sep$^-$ mutant strains compared with a strain carrying the equivalent construct producing a wild-type MinD protein (Fig. 3A, strain 2885). The filamentous phenotype was relatively mild in strain 2911 (D185A; Fig. 3B) but was particularly striking in strains 2915 (N165Y; Fig. 3C) and 2927 (A123P; Fig. 3E), indicating that some of the substitutions have a stronger effects than others. We also observed a small number of minicells, indicating that division was not totally inhibited at the poles (as is typical of *divIVA* null mutants; Reeve *et al*., 1973; Edwards and Errington, 1997). These observations would be consistent with the production of mutant MinD proteins that allow inhibition of division but are not properly topologically regulated.

To examine the topological regulation of the division inhibitor in the Sep$^-$ mutants, we analysed MinC localization using the *gfp–minC* fusion that these strains carry under the control of P_{xyl}. Fluorescence microscopy of exponentially growing cells in the presence of xylose showed that GFP–MinC was not properly targeted to the cell poles, although prominent bands of GFP were evident at irregular intervals along the length of the cell filaments, probably corresponding to sites where residual cell divisions had occurred or were occurring (Fig. 4). Some of the strong bands were in doublets, probably corresponding to sites of minicell formation, or were localized in minicells, as mentioned above (e.g. arrows in Fig. 4C and D). The signal was reminiscent of that of GFP–MinD in these mutants (see below) and strikingly different from that of GFP–MinC in the Min$^-$ mutants (compare with Fig. 2D), consistent with MinC still being under the control of MinD. In addition to the strong bands, some fainter bands of GFP–MinC were evident at intermediate positions, possibly corresponding to potential division sites (arrowheads). We reported previously that MinCD has an affinity for division sites independent of DivIVA (Marston and Errington, 1999). Presumably, this reflects an interaction between MinCD and the division machinery associated with the activity of MinCD in preventing division. (The irregular spacing of these bands could result from the loss of regulation of FtsZ ring formation as a result of repeated failure of rings to form and mature into sites of active division.) In general, the localization pattern of the mutants, particularly the release of the protein from the completed cell poles, was similar to that of GFP–MinC in a *divIVA* null mutant (Marston and Errington, 1999),

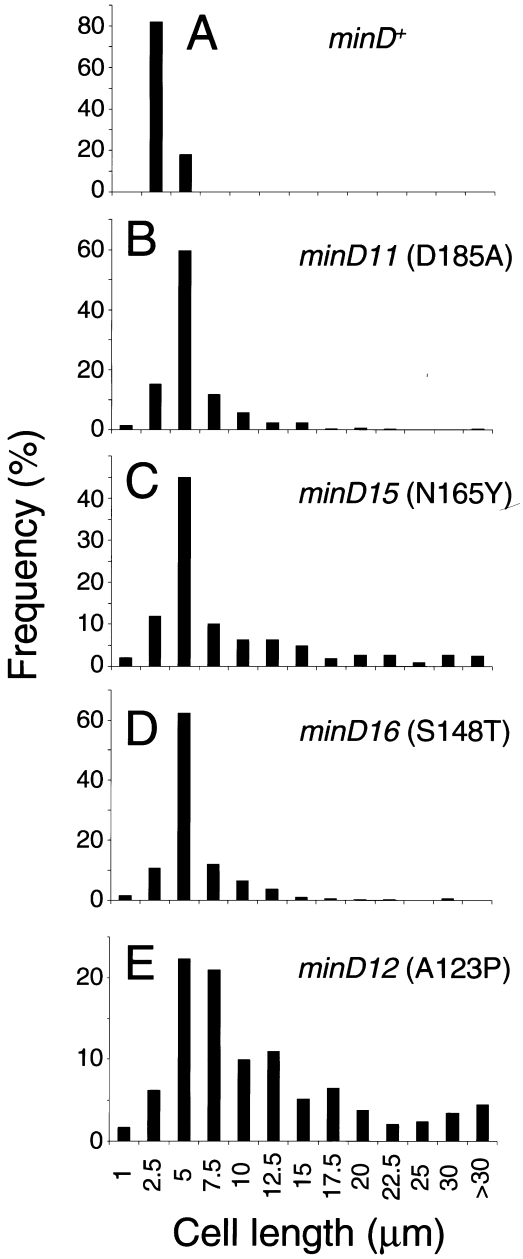

Fig. 3. The Sep$^-$ mutants form filaments. Cells were grown to exponential phase (OD_{600} of 0.4) in S medium containing 0.5% xylose and ethanol fixed. About 300 cells of each genotype were measured by digital analysis of phase-contrast images. The wild type (A, strain 2885) is compared with the four Sep$^-$ mutants: 2911 (B), 2915 (C), 2916 (D) and 2927 (E).

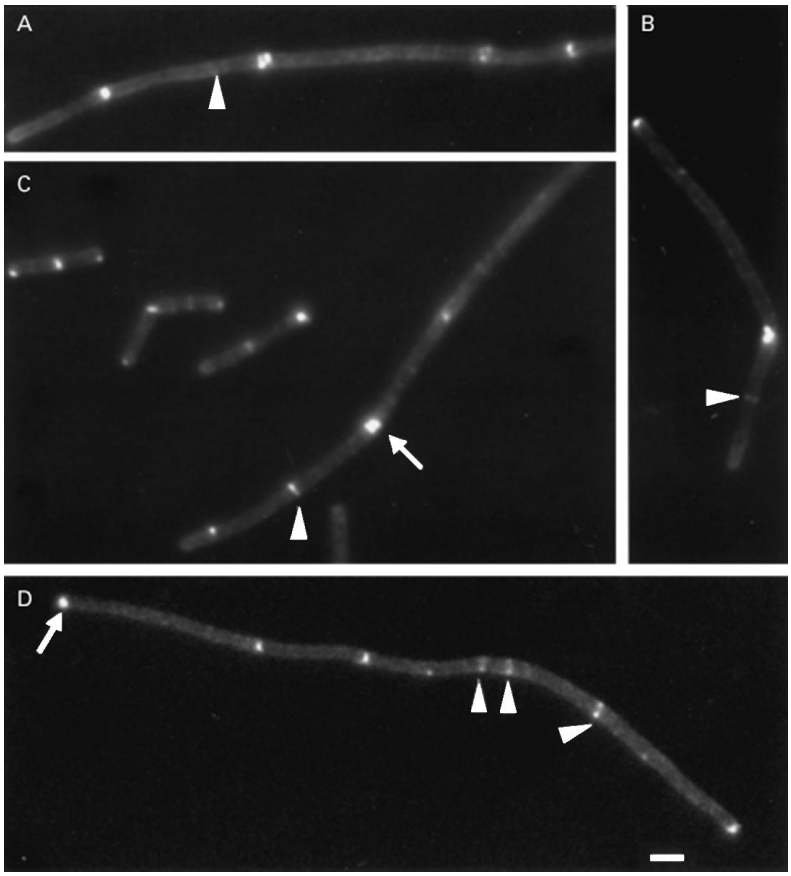

Fig. 4. GFP–MinC is not localized to the poles in the Sep$^-$ mutants. Cells from strains 2915 (A; MinD-N165Y), 2911 (B; MinD-D185A), 2916 (C; MinD-S148T) and 2927 (D; MinD-A123P) were grown to exponential phase (OD_{600} of 0.6–0.7) in S medium containing 0.5% xylose. Samples were taken for fluorescence microscopic imaging of the GFP. Arrows indicate minicells and arrowheads internal bands. Scale bar = 2 μm.

strongly suggesting that MinD retained its ability to interact with MinC but was impaired in its interaction with DivIVA.

To confirm that the phenotype observed in the Sep$^-$ mutants resulted from an improper localization of the mutant MinD protein, we examined GFP–MinD localization directly for MinD-S148T and MinD-N165Y. Plasmids carrying *minD* with the corresponding mutations were recovered from the chromosomes of strain 2915 and 2916 (see *Experimental procedures*). They were then introduced by single cross-over integration into strain 1981, carrying a *gfp–minD* fusion under the control of P_{xyl}. The resulting strains were grown to exponential phase in the presence of xylose, and the cells were examined by fluorescence microscopy. As expected, GFP–MinD-S148T and GFP–MinD-N165Y produced a relatively delocalized signal with only weak targeting or retention of the protein at the cell poles (Fig. 5A and B). As for GFP–MinC, stronger internal bands were present, probably corresponding to nascent division sites that had escaped inhibition by MinCD, and some fainter internal bands (arrowheads), probably corresponding to potential division sites at which inhibition of division was actively occurring. Again, the localization was very similar to that of wild-type GFP–MinD in a *divIVA* null mutant (Fig. 5C). As for GFP–MinC, these observations would be consistent with the mutant MinD proteins retaining some affinity for the division apparatus and only being defective in their interaction with DivIVA.

Taken together, these results indicate that the inhibition of cell division throughout the cell in the Sep$^-$ mutants results from improper localization of MinD, leading to localization and activation of the division inhibitor MinC not only at the poles but also elsewhere in the cell. The results also showed that it is possible to separate the activities of MinD involved in its positioning from those involved in the interaction with MinC.

Discussion

Phenotype of minD *mutants predicted to be affected in nucleotide binding or hydrolysis*

We have constructed several mutant strains carrying mutations in the ATPase domain of MinD. In all these mutants, MinD seems to be totally inactive and delocalized, although it retains some affinity for the cell membrane. The interaction with MinC, which appears no longer to be associated with the cell membrane, is probably disrupted. Several mutations in the ATP-binding

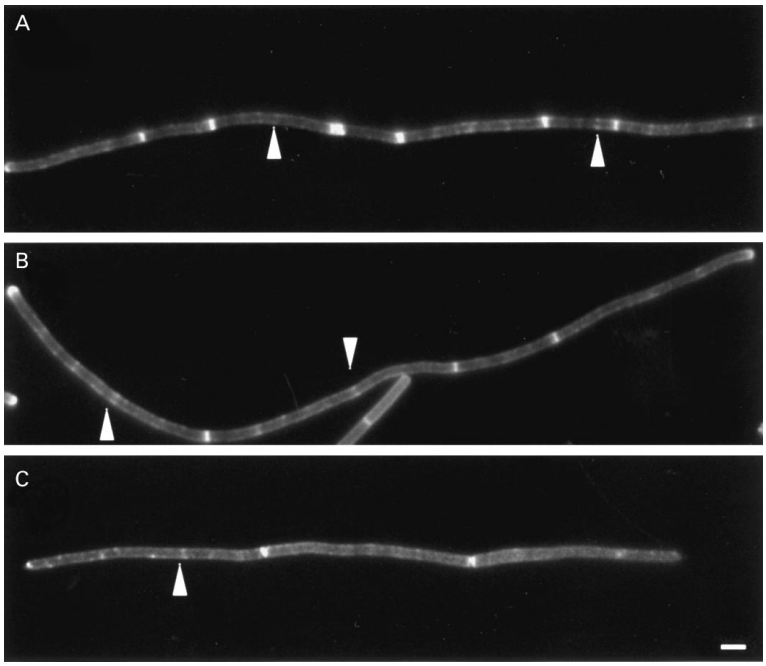

Fig. 5. GFP–MinD is not properly localized in the Sep$^-$ mutants. Cells from strains 2918 (A; MinD-N165Y), 2919 (B; MinD-S148T) and (C; MinD$^+$, *ΔdivIVA*) were grown to exponential phase (OD_{600} of 0.6–0.7) in S medium containing 0.5% xylose. Samples were taken for fluorescence microscopic imaging of the GFP. Arrowheads indicate internal GFP–MinD bands. Scale bar = 2 μm.

domain of *E. coli* MinD (among which lysine to alanine at amino acid 16) have been shown to affect the capacity of the protein to activate MinC (de Boer *et al*., 1991), but the localization of these mutant proteins has not been reported. The inability of our mutants to activate MinC could reflect the failure to position and concentrate this protein at the membrane, which is thought to be the basis for MinC activation by MinD (Hu *et al*., 1999; Raskin and De Boer, 1999a). Three of the mutations that we introduced are likely to interfere with nucleotide binding, consistent with this being essential for MinD activity. The fourth substitution, G12V, was designed to alter nucleotide hydrolysis. When the same substitution was introduced into Soj, a distant relative of MinD, the protein still localized, but it no longer showed any dynamic behaviour (Quisel *et al*., 1999). There are several possible explanations for the fact that MinD-G12V is delocalized and inactive. First, nucleotide binding might be impaired in this protein, in which case this mutant is analogous to the other three Min$^-$ mutants. Secondly, MinD-G12V might be a hyperactive ATPase, in which case MinD would mainly be in the ADP-bound state. This would imply that MinD-ADP is unable to localize. Thirdly, this protein might bind ATP but be defective in hydrolysis. In this case, MinD-ATP would be unable to localize to the poles, possibly because it cannot self-assemble (see *Introduction* and below). According to either of the latter models, nucleotide hydrolysis, and not only nucleotide binding, would be necessary for MinD activity. It should also be noted that we cannot exclude the possibility that the mutations we have constructed simply disrupt the three-dimensional structure of the protein in a relatively non-specific manner.

MinD *mutants affected in interaction with DivIVA*

According to our model for the operation of the Min system in *B. subtilis*, DivIVA anchored at the cell poles interacts with MinD to recruit it (and consequently MinC) to the polar regions. If this model were correct, it should be possible to obtain mutations in *minD* that leave intact its ability to interact with MinC and promote inhibition of division but block its interaction with DivIVA and, therefore, the restriction of division inhibition to the cell poles. To our knowledge, this class of mutation has not been obtained with the *E. coli* system, but we were able to obtain them for *B. subtilis*. Four different Sep$^-$ mutants were isolated and, in each case, the phenotype was consistent with the model: the localization patterns observed for both MinD and MinC fusions to GFP were similar to those described previously for *divIVA* null mutants (Marston *et al*., 1998; Marston and Errington, 1999). The similarity included both the loss of retention of MinCD at the cell poles and the residual enrichment at nascent and potential division sites (Marston *et al*., 1998; Marston and Errington, 1999). Formally, we cannot exclude a model in which MinCD leaves the cell poles in the mutants because it has an increased general affinity for the division machinery. However, as the interaction with the division machinery is thought to take place through MinC, at least in *E. coli* (de Boer *et al*., 1990; Hu *et al*., 1999), and the mutations lie in *minD*, we do not currently favour this model.

The Sep$^-$ mutants all had substitutions in the mid- to C-terminal part of the protein, raising the possibility that this constitutes a domain or surface involved in the putative interaction with DivIVA. The sequence of

B. subtilis MinD could readily be aligned with that of *E. coli* and with those of the two organisms for which MinD structures have recently been solved: *A. fulgidus* (Cordell and Löwe, 2001) and *P. furiosus* (Hayashi *et al.*, 2001) (Fig. 1). Comparison of the alignments and the structures suggests that the secondary structural elements are highly conserved. On this basis, three of the substitutions we found (corresponding to *A. fulgidus* residues labelled Ser-144, Leu-159 and Ile-176) lie in or near helices H5 and H6 [according to the nomenclature of Cordell and Löwe (2001)] (Fig. 6). These residues lie near each other on one side of the protein and may therefore comprise part of a region involved in the interaction with DivIVA. Two of the residues are actually located in loops just adjacent to the helices. This is not uncommon for amino acids involved in protein–protein interactions (for example, see Williams *et al.*, 1997), but the relatively unconserved nature of these loops makes it difficult to make firm predictions about the precise configuration of the relevant residues in the *B. subtilis* MinD protein.

The substitution at A123 (corresponding to Ala-119 of *A. fulgidus* MinD in Fig. 6) is not far distant in three-dimensional terms from the other substitutions, again suggesting a potential region of contact with DivIVA. However, this substitution is particularly interesting, because it is highly conserved, lying in the 'switch II' region of the protein (Fig. 1). In the *P. furiosus* structure, the equivalent residue (A121) is thought to have a role in the catalysis of ATP hydrolysis because the backbone N of this residue makes a hydrogen bond with a water molecule that is aligned in such a way that it could make an in-line nucleophilic attack on the γ-phosphate of ATP (Hayashi *et al.*, 2001). We suggest that DivIVA may use a contact with this alanine to regulate nucleotide hydrolysis. By analogy with the regulation of actin polymerization (Schmidt and Hall, 1998), we speculate that DivIVA could act as a 'capping' protein to stabilize the self-assembly (possibly ATP dependent) of MinD oligomers at the cell pole. This would provide a mechanism for sequestering the MinCD inhibitor to the cell poles. In extensive time lapse experiments (M. El Karoui, unpublished), we have not detected an oscillatory behaviour for MinD, as has been described for *E. coli* (Raskin and de Boer 1999b; Rowland *et al.*, 2000). The distinction between the two systems may lie in the MinE protein, which differs from DivIVA in being mobile, but which we suggest could also use nucleotide hydrolysis to control MinD assembly/disassembly to bring about oscillation. *In vitro* experiments with the purified proteins will be required to test this model but, so far, the *B. subtilis* proteins have proved refractory to purification in an active form.

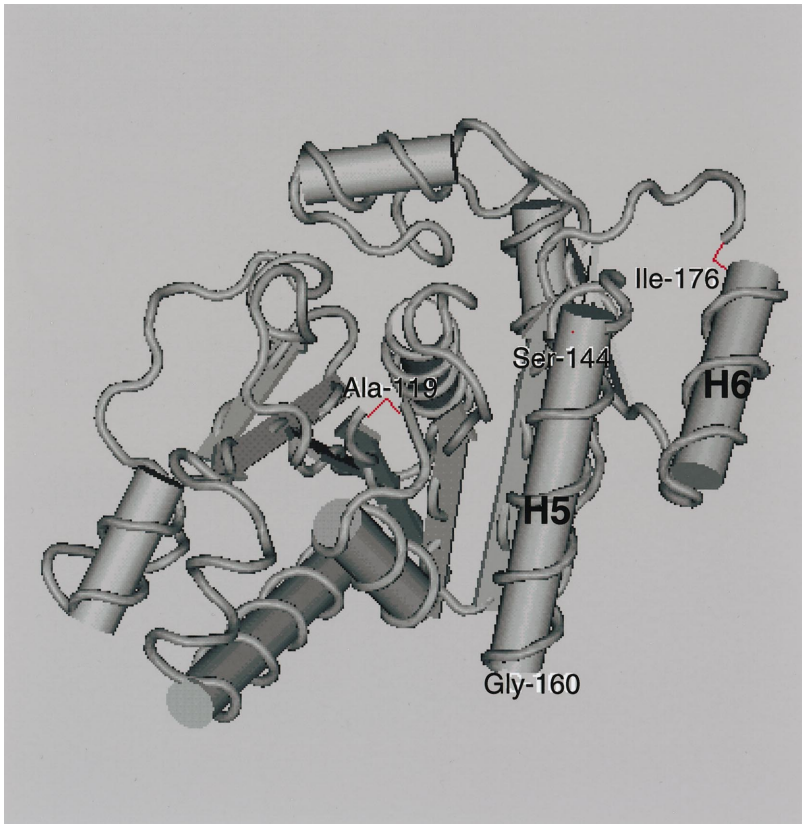

Fig. 6. Structure of MinD from *A. fulgidus* showing various secondary structural features, and with residues corresponding to those affected by the Sep$^-$ mutations of *B. subtilis minD* labelled. H5 and H6 refer to α-helices as defined by Cordell and Löwe (2001).

Experimental procedures

Bacterial strains and plasmids

Bacillus subtilis strains and plasmids used in this study are listed in Table 1. All cloning was carried out in *E. coli* MC1061 (Wertman *et al*., 1986), except for vector pSG4820, in which case *E. coli* DH5α (Gibco BRL) was used. To construct plasmid pSG4801, a 0.7 kb DNA fragment containing the *minD* gene was amplified by PCR using primers AM1 (5′-gggaggaactcgagttgggtgaggc-3′) and AM2 (5′-gattcttctcttgaat tctatcatcacattaag-3′), introducing *Xho*I and *Eco*RI sites respectively. The *Eco*RI–*Xho*I fragment was inserted between these sites in vector pSG1301. pSG4815 and pSG4816 were obtained by digesting chromosomal DNA from strains 2915 and 2916 with *Acc*65I, ligating in diluted conditions and transforming into *E. coli*. To construct pSG4820, a 1.4 kb DNA fragment containing the *minC and minD* genes was amplified by PCR from strain 2912 using primers AM15 (5′-cctgtccacacaatctgc-3′) and OM27 (5′-ttagc cgaattcttaagatctttactccgaaaaatg-3′), introducing *Xho*I and *Eco*RI sites respectively. The *Eco*RI–*Xho*I fragment was inserted between these sites in pSG1729.

General methods

Bacillus subtilis cultures were grown in S medium supplemented with tryptophan (20 μg ml^{-1}) and hydrolysed casein as described by Marston *et al*. (1998). When necessary, 0.5% xylose was added. *B. subtilis* strains were transformed according to the method of Anagnostopoulos and Spizizen (1961) as modified by Jenkinson (1983). Transformants were selected on Oxoid nutrient agar containing, as necessary, chloramphenicol (5 μg ml^{-1}) or spectinomycin (50 μg ml^{-1}). DNA manipulations and *E. coli* transformations were carried out by standard methods (Sambrook *et al*., 1989).

Table 1. *B. subtilis* strains and plasmids.

Strain or plasmid	Relevant characteristic[a]	Source/construction
B. subtilis		
SG38	*trpC2 amyE*	Errington and Mandelstam (1983)
1981	*trpC2 Ω(minD::erm)1901 Ω(amyE::spc P_{xyl}-gfp−minD)1730*	Marston *et al.* (1998)
1984	*trpC2 Ω(minD::erm)1901 divIVA::tet Ω(amyE::spc P_{xyl}-gfp−minD)1730*	Marston *et al.* (1998)
2770	*trpC2 ΔminCD::erm*	A. Leung (unpublished)
2867	As SG38, *minD*::pSG4804 (*minD1 cat*) (K16A)	pSG4804→SG38 (Cm^R)
2868	As SG38, *minD*::pSG4805 (*minD2 cat*) (D38A)	pSG4805→SG38 (Cm^R)
2869	As SG38, *minD*::pSG4806 (*minD3 cat*) (D120A)	pSG4806→SG38 (Cm^R)
2870	As SG38, *minD*::pSG4807 (*minD4 cat*) (V142A)	pSG4807→SG38 (Cm^R)
2871	As SG38, *minD*::pSG4808 (*minD5 cat*) (N174A)	pSG4808→SG38 (Cm^R)
2880	As 2895, *minD*::pSG4804 (*minD1 cat*) (K16A)	pSG4804→2895 (Cm^R)
2885	As 2895, *minD*::pSG4801 (*minD$^+$ cat*)	pSG4801→2895 (Cm^R)
2888	As 2896, *minD*::pSG4804 (*minD1* cat) (K16A)	pSG4804→2896 (Cm^R)
2893	As 2896, *minD*::pSG4801 (*minD$^+$* cat)	pSG4801→2896 (Cm^R)
2895	*trpC2 ΔminCD::erm Ω(amyE::spc P_{xyl}-gfp−minC minD)1736*	pSG1736→2770 (Spc^R)
2896	*trpC2 ΔminCD::erm Ω(amyE::spc P_{xyl}-gfp−minD*)1730	pSG1730→2770 (Spc^R)
2908	As SG38, *minD*::pSG4811 (*minD6 cat*) (G12V)	pSG4811→SG38 (Cm^R)
2911	As 2895, *minD*::pSG4801^{mut} (*minD11 cat*) (D185A)	pSG4801^{mut}→2895 (Cm^R)
2912	As 2895, *minD*::pSG4801^{mut} (*minD12 cat*) (A123P)	pSG4801^{mut}→2895 (Cm^R)
2915	As 2895, *minD*::pSG4801^{mut} (*minD15 cat*) (N165Y)	pSG4801^{mut}→2895 (Cm^R)
2916	As 2895, *minD*::pSG4801^{mut} (*minD16 cat*) (S148T)	pSG4801^{mut}→2895 (Cm^R)
2918	As1981, *minD*::pSG4815 (*minD15 cat*) (N165Y)	pSG4815→1981 (Cm^R)
2919	As1981, *minD*::pSG4816 (*minD16 cat*) (S148T)	pSG4816→1981 (Cm^R)
2927	As 2770, *Ω(amyE::spc P_{xyl}-gfp-minC minD12)4820* (A123P)	pSG4820→2770 (Spc^R)
Plasmids		
pSG1301	*bla cat*. Integration plasmid	Stevens *et al*. (1992)
pSG1729	*bla amyE3′ spc P_{xyl}-gfp amyE5′*	Lewis and Marston (1999)
pSG1730	*bla amyE3′ spc P_{xyl}-gfp−minD amyE5′*	Marston *et al*. (1998)
pSG1736	*bla amyE3′ spc P_{xyl}-gfp−minC minD amyE5′*	Marston and Errington (1999)
pSG4801	*bla cat minD$^+$*	This work
pSG4801^{mut}	*bla cat minD^{mut}*	Random mutagenesis
pSG4804	*bla cat minD1* (K16A)	Site-directed mutagenesis
pSG4805	*bla cat minD2* (D38A)	Site-directed mutagenesis
pSG4806	*bla cat minD3* (D120A)	Site-directed mutagenesis
pSG4807	*bla cat minD4* (V142A)	Site-directed mutagenesis
pSG4808	*bla cat minD5* (N174A)	Site-directed mutagenesis
pSG4811	*bla cat minD6* (G12V)	Site-directed mutagenesis
pSG4815	*bla cat minD15* (N165Y)	Plasmid rescued from strain 2915
pSG4816	*bla cat minD16* (S148T)	Plasmid rescued from strain 2916
pSG4820	*bla amyE3′ spc P_{xyl}-gfp-minC minD12 amyE5′*	This work

a. Note that *minD*::pSG4804 (*minD1 cat*)(K16A), for example, means that the non-replicating plasmid pSG4804 has integrated into the *minD* gene of the recipient strain by single cross-over (selected using the chloramphenicol resistance gene, *cat*) and that the site of crossing over was such that the *minD1allele* (which carries the K16A amino acid change) is expressed, rather than the wild-type allele.

Site-directed mutagenesis of minD

Plasmid pSG4801 DNA (0.3 ng μl^{-1}) was amplified by PCR (with *Pfu* polymerase), using one primer containing the desired mutation and a reverse primer (not complementary) with its 5′ extremity precisely one base before the 5′ end of the mutagenic primer. A linear product of the size of the plasmid was purified on a 0.7% agarose gel. Approximately 100 ng of the purified PCR product was incubated with ATP (3 mM), 1 unit of T4 polynucleotide kinase and 1 unit of DNA ligase in ligase buffer (total volume 30 ml) overnight at room temperature. A 15 μl sample of the reaction was used to transform *E. coli* strain MC1061. The presence of the mutation was checked by DNA sequencing using a departmental service. The resulting plasmids were introduced by single cross-over into the relevant strains, and the integrations were checked by PCR and sequencing.

Random mutagenesis of minD

A 0.7 kbp fragment containing the *minD* gene was amplified using primers AM1 and AM2 with *Taq* polymerase in mutagenic conditions. The balance of the dinucleotides was altered (200 μM dGTP and dATP and 1 mM dCTP and dTTP), the concentration of magnesium chloride was increased (6.25 mM) and the following programme was used: 1 min at 95°C, 1 min at 45°C and 1 min 30 s at 72°C for 30 cycles. The mutagenized *Eco*RI–*Xho*I DNA fragment was ligated to *Eco*RI–*Xho*I-digested pSG1301 and transformed into *E. coli* strain MC1061. All the ampicillin-resistant transformants were collected and inoculated into 100 ml of 2× TY medium. Cells were grown overnight, harvested and used to isolate plasmid DNA (called pSG4801^{mut}). pSG4801^{mut} DNA was used to transform strain 2895 by single cross-over, and chloramphenicol-resistant transformants showing a growth defect in the presence of xylose were chosen. To evaluate the mutagenesis rate, we also transformed pSG4801^{mut} into the wild-type strain SG38 and counted the number of minicell-producing colonies, thus obtaining a rough estimate of the percentage of transformants in which *minD* was mutated (because the protein was either inactive or not produced). This percentage was ≈3%. To construct strain 2927, pSG4820 was transformed by double cross-over into SG38 at the *amyE* locus.

Subcellular localization experiments and cell length analysis

The relevant strains were grown overnight, either in S medium without xylose or on nutrient agar plates with the appropriate antibiotic and 0.5% xylose. The following morning, each strain was inoculated into warm S medium containing 0.5% xylose to give a final OD_{600} of 0.1. All cultures were grown at 30°C until they reached an OD_{600} of 0.7–0.8, when samples were taken for microscopy. For cell length analysis, the strains were grown as described above, except that samples were taken when the cultures reached an OD_{600} of 0.4, and the cells were ethanol fixed as described previously (Hauser and Errington, 1995).

Microscopy

The subcellular localization patterns of GFP–MinD and GFP–MinC were examined in live cells on agarose slides (1.2% in water) as described by Glaser *et al.* (1997) For cell length analysis, ethanol-fixed cells were also examined on agarose slides. Images were acquired and analysed with a Princeton Instruments Micromax 1300Y/HS CDD camera and METAMORPH version 3.6 software. Final images were assembled using Adobe PHOTOSHOP version 5.5.

Acknowledgements

This work was supported by a grant from the Biotechnology and Biological Sciences Research Council. M.E.K. was the recipient of an EMBO long-term fellowship, reference number ALTF 209-1999. J.E. is the recipient of a BBSRC Senior Research Fellowship. We thank Alice Taylor for DNA sequencing, and Adele Marston for strains and helpful discussions.

References

Adler, H.I., Fisher, W.D., Cohen, A., and Hardigree, A.A. (1967) Miniature *Escherichia coli* cells deficient in DNA. *Proc Natl Acad Sci USA* **57**: 321–326.

Anagnostopoulos, C., and Spizizen, J. (1961) Requirements for transformation in *Bacillus subtilis*. *J Bacteriol* **81**: 741–746.

Barák, I., Prepiak, P., and Schmeisser, F. (1998) MinCD proteins control the septation process during sporulation of *Bacillus subtilis*. *J Bacteriol* **180**: 5327–5333.

de Boer, P.A.J., Crossley, R.E., and Rothfield, L.I. (1989) A division inhibitor and a topological specificity factor coded for by the minicell locus determine proper placement of the division septum in *E. coli*. *Cell* **56**: 641–649.

de Boer, P.A.J., Crossley, R.E., and Rothfield, L.I. (1990) Central role for the *Escherichia coli minC* gene product in two different cell division-inhibition systems. *Proc Natl Acad Sci USA* **87**: 1129–1133.

de Boer, P.A.J., Crossley, R.E., Hand, A.R., and Rothfield, L.I. (1991) The MinD protein is a membrane ATPase required for the correct placement of the *Escherichia coli* division site. *EMBO J* **10**: 4371–4380.

Cha, J.-H., and Stewart, G.C. (1997) The *divIVA* minicell locus of *Bacillus subtilis*. *J Bacteriol* **179**: 1671–1683.

Chen, C.M., Misra, T.K., Silver, S., and Rosen, B.P. (1986) Nucleotide sequence of the structural genes for an anion pump. The plasmid-encoded arsenical resistance operon. *J Biol Chem* **261**: 15030–15038.

Cordell, S.C., and Löwe, J. (2001) Crystal structure of the bacterial cell division regulator MinD. *FEBS Lett* **492**: 160–165.

Edwards, D.H., and Errington, J. (1997) The *Bacillus subtilis* DivIVA protein targets to the division septum and controls the site specificity of cell division. *Mol Microbiol* **24**: 905–915.

Errington, J., and Mandelstam, J. (1983) Variety of sporulation phenotypes resulting from mutations in a single regulatory locus, *spoIIA*, in *Bacillus subtilis*. *J Gen Microbiol 129*: 2091–2101.

Fu, X., Shih, Y.L., Zhang, Y., and Rothfield, L.I. (2001) The MinE ring required for proper placement of the division site is a mobile structure that changes its cellular location during

the *Escherichia coli* division cycle. *Proc Natl Acad Sci USA* **98**: 980–985.
Gérard, E., Labedan, B., and Forterre, P. (1998) Isolation of a *minD*-like gene in the hyperthermophilic archaeon *Pyrococcus* AL585, and phylogenetic characterization of related proteins in the three domains of life. *Gene* **222**: 99–106.
Glaser, P., Sharpe, M.E., Raether, B., Perego, M., Ohlsen, K., and Errington, J. (1997) Dynamic, mitotic-like behaviour of a bacterial protein required for accurate chromosome partitioning. *Genes Dev* **11**: 1160–1168.
Hale, C.A., Meinhardt, H., and de Boer P.A.J. (2001) Dynamic localization cycle of the cell division regulator MinE in *Escherichia coli*. *EMBO J* **20**: 1563–1572.
Hauser, P.M., and Errington, J. (1995) Characterization of cell cycle events during the onset of sporulation in *Bacillus subtilis*. *J Bacteriol* **177**: 3923–3931.
Hayashi, I., Oyama, T., and Morikawa, K. (2001) Structural and functional studies of MinD ATPase: implications for the molecular recognition of the bacterial cell division apparatus. *EMBO J* **20**: 1819–1828.
Hiraga, S. (2000) Dynamic localization of bacterial and plasmid chromosomes. *Annu Rev Genet* **34**: 21–59.
Hu, Z., and Lutkenhaus, J. (1999) Topological regulation of cell division in *Escherichia coli* involves rapid pole to pole oscillation of the division inhibitor MinC under the control of MinD and MinE. *Mol Microbiol* **34**: 82–90.
Hu, Z., Mukherjee, A., Pichoff, S., and Lutkenhaus, J. (1999) The MinC component of the division site selection system in *Escherichia coli* interacts with FtsZ to prevent polymerization. *Proc Natl Acad Sci USA* **96**: 14819–14824.
Huang, J., Cao, C., and Lutkenhaus, J. (1996) Interaction between FtsZ and inhibitors of cell division. *J Bacteriol* **178**: 5080–5085.
Jenkinson, H.F. (1983) Altered arrangement of proteins in the spore coat of a germination mutant of *Bacillus subtilis*. *J Gen Microbiol* **129**: 1945–1958.
Koonin, E.V. (1993) A superfamily of ATPases with diverse functions containing either classical or deviant ATP-binding motif. *J Mol Biol* **229**: 1165–1174.
Lee, S., and Price, C.W. (1993) The *minCD* locus of *Bacillus subtilis* lacks the *minE* determinant that provides topological specificity to cell division. *Mol Microbiol* **7**: 601–610.
Levin, P.A., Margolis, P.S., Setlow, P., Losick, R., and Sun, D. (1992) Identification of *Bacillus subtilis* genes for septum placement and shape determination. *J Bacteriol* **174**: 6717–6728.
Lewis, P.J., and Marston, A.L. (1999) GFP vectors for controlled expression and dual labelling of protein fusions in *Bacillus subtilis*. *Gene* **227**: 101–109.
Lutkenhaus, J., and Addinall, S.G. (1997) Bacterial cell division and the Z ring. *Annu Rev Biochem* **66**: 93–116.
Marston, A.L., and Errington, J. (1999) Selection of the midcell division site in *Bacillus subtilis* through MinD-dependent polar localization and activation of MinC. *Mol Microbiol* **33**: 84–96.
Marston, A.L., Thomaides, H.B., Edwards, D.H., Sharpe, M.E. and Errington, J. (1998) Polar localization of the MinD protein of *Bacillus subtilis* and its role in selection of the mid-cell division site. *Genes Dev* **12**: 3419–3430.
Quisel, J.D., Lin, D.C.-H., and Grossman, A.D. (1999) Control of development by altered localization of a transcription factor in *B. subtilis*. *Mol Cell* **4**: 665–672.
Raskin, D.M., and De Boer, P.A.J. (1999a) MinDE-dependent pole-to-pole oscillation of division inhibitor MinC in *Escherichia coli*. *J Bacteriol* **181**: 6419–6424.
Raskin, D.M., and De Boer, P.A.J. (1999b) Rapid pole-to-pole oscillation of a protein required for directing division to the middle of *Escherichia coli*. *Proc Natl Acad Sci USA* **96**: 4971–4976.
Reeve, J.N., Mendelson, N.H., Coyne, S.I., Hallock, L.L., and Cole, R.M. (1973) Minicells of *Bacillus subtilis*. *J Bacteriol* **114**: 860–873.
Rowland, S.L., Fu, X., Sayed, M.A., Zhang, Y., Cook, W.R., and Rothfield, L.I. (2000) Membrane redistribution of the *Escherichia coli* MinD protein induced by MinE. *J Bacteriol* **182**: 613–619.
Sambrook, J., Fritsch, E.F., and Maniatis, T. (1989) *Molecular Cloning: A Laboratory Manual*, 2nd edn. Cold Spring Harbor, NY: Cold Spring Harbor Laboratory Press.
Schmidt, A., and Hall, M.N. (1998) Signalling to the actin cytoskeleton. *Annu Rev Cell Dev Biol* **14**: 305–338.
Stevens, C.M., Daniel, R., Illing, N., and Errington, J. (1992) Characterization of a sporulation gene, *spoIVA*, involved in spore coat morphogenesis in *Bacillus subtilis*. *J Bacteriol* **174**: 586–594.
Story, R.M., and Steitz, T.A. (1992) Structure of the recA protein–ADP complex. *Nature* **355**: 374–376.
Teather, R.M., Collins, J.F., and Donachie, W.D. (1974) Quantal behaviour of a diffusible factor which initiates septum formation at potential division sites in *Escherichia coli*. *J Bacteriol* **118**: 407–413.
Thompson, J.D., Higgins, D.G., and Gibson, T.J. (1994) CLUSTAL W: improving the sensitivity of progressive multiple sequence alignment through sequence weighting, position-specific gap penalties and weight matrix choice. *Nucleic Acids Res* **22**: 4673–4680.
Vogel, U.S., Dixon, R.A., Schaber, M.D., Diehl, R.E., Marshall, M.S., Scolnick, E.M., *et al.* (1988) Cloning of bovine GAP and its interaction with oncogenic ras p21. *Nature* **335**: 90–93.
Walker, J.E., Saraste, M., Runswick, M.J., and Gay, N.J. (1982) Distantly related sequences in the α- and β-subunits of ATP synthase, myosin, kinases and other ATP-requiring enzymes and a common nucleotide binding fold. *EMBO J* **1**: 945–951.
Wertman, K.F., Wyman, A.R., and Botstein, D. (1986) Host/vector interactions which affect the viability of recombinant phage lambda clones. *Gene* **49**: 253–262.
Williams, S.M., Savery, N.J., Busby, S.J., and Wing, H.J. (1997) Transcription activation at class I FNR-dependent promoters: identification of the activating surface of FNR and the corresponding contact site in the C-terminal domain of the RNA polymerase alpha subunit. *Nucleic Acids Res* **25**: 4028–4034.
Zhou, T., and Rosen, B.P. (1999) Asp45 is a $Mg2+$ ligand in the ArsA ATPase. *J Biol Chem* **274**: 13854–13858.
Zhou, T., Radaev, S., Rosen, B.P., and Gatti, D.L. (2000) Structure of the ArsA ATPase: the catalytic subunit of a heavy metal resistance pump. *EMBO J* **19**: 4838–4845.